Journal of Applied Analysis and Computation
Volume *, Number *, * *, 1–13
Website:http://www.jaac-online.com
DOI:10.11948/***

A HERMITE FINITE ELEMENT METHOD FOR THE VIBRATION PROBLEM OF THE RAYLEIGH-BISHOP BEAM

Yi Gong†

Abstract In this paper, a Hermite finite element method is proposed for the Rayleigh-Bishop equation which describes the vibration problem of the Rayleigh-Bishop beam. We first present the semi-discrete Galerkin finite element form for the Rayleigh-Bishop equation. Then by means of the cubic Hermite element, a full-discrete finite element scheme is established. Furthermore, a numerical algorithm based on the Hermite finite element method is proposed to solve the fourth-order Rayleigh-Bishop equation. Finally, a numerical example is given to illustrate the effectiveness of the proposed method. The Hermite finite element method is potentially applied to other vibration problems.

Keywords Rayleigh-Bishop beam, Pseudohyperbolic equation, Hermite finite element.

MSC(2010) 35L82, 65N30.

1. Introduction

During the last decade, the vibration problems of the beam have attracted considerable attention since its wide presence in various fields including mechanical engineering, bridge construction, aerospace and so on [1]. The equations for the transverse vibration of beams usually are in the form of fourth-order partial differential equations with two boundary conditions at each end, which is difficult to find an analytical solution [2, 3]. Numerical methods provide a powerful framework for obtaining approximate solutions to the vibration problems of the beams. There are many valuable results [4–10] about numerical methods for the vibration problems of the viscoelastic beams.

In particular, the finite element method has been employed successfully in the analysis of viscoelastic beams by many researchers [11–20]. In Reference [12], the dynamic model of Euler-Bernoulli beams is studied by using the finite element method. And an iterative solution algorithm based the two-dimensional finite element method is proposed to obtain beam displacements. In Reference [13], a mixed finite element method is proposed to solve three-field (displacement, strain, stress) variational formula for beams. In Reference [14], a three-dimensional finite element method is used to study the viscoelastic panel with axial and transverse load, which is also applicable to viscoelastic beams. In Reference [15], an effective nu-

†Department of Basic Courses, Shanghai Customs College, Shanghai 201204, China.
Email: gongyi@shcc.edu.cn (Y. Gong)

merical method based on nonlocal two-noded finite elements is proposed, by which the stress-driven solution can be obtained by using only one two-noded element. In Reference [16], an enriched hierarchical one-dimensional finite element method is presented, which can be used to study the rheological behavior of thick arbitrarily laminated beams. In Reference [17], a scheme for the vibration equation of the viscoelastic beam is developed by using the Hermite finite element. The cubic Hermite element can guarantee the continuity of the first derivative of the interpolation function. In Reference [18], a finite element method is proposed for the static and free vibration analyses of sandwich beams. In the above literature [12–18], the influence of the rotatory inertia of the cross-section is not taken into account. The beam model considering the rotatory inertia of the cross-section is a high-order partial differential equation with the mixed partial derivative with respect to time and space, i.e. the Rayleigh-Bishop model [21, 22], which belongs to the pseudohyperbolic equation [23–27]. It has been shown [28] that the Rayleigh-Bishop model improves on estimations made by the classical Euler-Bernoulli equation. The Rayleigh-Bishop model makes it possible to analyse longitudinal wave propagation in beams that are relatively thick due to the inclusion of transverse effects in the model. However, there is little work about the finite element method for the vibration problem of the Rayleigh-Bishop beam.

Motivated by the above observations, we present a Hermite finite element method for the vibration problem of the Rayleigh-Bishop beam. This numerical method is used to obtain the transverse displacement of the Rayleigh-Bishop beam with fixed ends. Based on the cubic Hermite element, a full-discrete finite element scheme is established, which can guarantee the continuity of the first derivative of the interpolation function. Finally, a numerical example is given to demonstrate the validity of the scheme.

The main contributions of this work are summarised as follows:

(1) We formulate a full-discrete finite element scheme for the Rayleigh-Bishop equation.

(2) An effective numerical algorithm based on the cubic Hermite element is developed to compute the transverse displacement of the Rayleigh-Bishop beam with fixed ends.

The rest of the paper is organized as follows. In Section 2, some basic definitions and the problem description are given. In Section 3, we propose a full-discrete finite element scheme to solve the Rayleigh-Bishop equation. In Section 4, a numerical example is given to illustrate the effectiveness of the proposed method. In Section 5, some conclusions are summarised.

2. Preliminaries

In this section, an one-dimensional fourth-order pseudohyperbolic equation is presented, which describes the vibration problem of a beam with fixed ends.

Consider the following vibration problem of the Rayleigh-Bishop beam [1]

$$EIw_{xxxx} + \rho S w_{tt} - \rho I w_{xxtt} - P w_{xx} = f(x,t), \quad x \in [0,l],\ t \in [0,T], \tag{2.1}$$

where $w(x,t)$ is the transverse displacement of the beam, E is Young's modulus, I is the second moment of cross-sectional area, EI denotes the bending stiffness, ρ

is the density of the beam, S is the cross-sectional area, ρS denotes the mass per unit length, ρI is the rotatory inertia of cross-sectional area, P is the coefficient of tension, l is the beam length, x is the axial coordinate and $f(x,t)$ is the smooth function which is known.

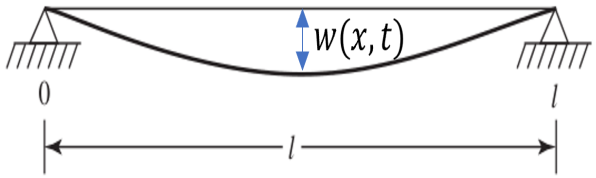

Figure 1. Schematic of a beam with fixed ends

We investigate the vibration problem of a beam with fixed ends, which is described by the following homogeneous boundary conditions

$$w(0,t) = w(l,t) = 0,\ w_{xx}(0,t) = w_{xx}(l,t) = 0,\ t \in [0,T], \tag{2.2}$$

The initial conditions of the system (2.1) is presented as follows

$$w(x,0) = \varphi(x),\ w_t(x,0) = \psi(x), x \in [0,l], \tag{2.3}$$

where $\varphi(x)$ and $\psi(x)$ are smooth functions which are known.

Remark 2.1. The dynamical model (2.1) and the boundary conditions (2.2) are derived by using the Hamilton's variational principle and the Rayleigh-Bishop theory [17]. The influence of rotatory inertia of the cross-section is taken into account but the shear deformation is neglected in the analysis. Compared with the Euler-Bernoulli beam which neglects the effect of inertia on modeling, the Rayleigh-Bishop beam makes it possible to analyse longitudinal wave propagation in beams that are relatively thick.

3. Finite Element Approximation

In this section, we first present the semi-discrete Galerkin finite element form for the Rayleigh-Bishop equation (2.1). Then, based on the cubic Hermite element, a full-discrete finite element scheme is established, which can guarantee the continuity of the first derivative of the interpolation function. Finally, a numerical algorithm based on the Hermite finite element method is proposed to solve the euqation (2.1) with the boundary conditions (2.2) and the initial conditions (2.3).

Let $I = [0,l]$. The definition of Sobolev space $H_0^2(I)$ is given as follows.

Definition 3.1. The Sobolev space $H_0^2(I)$ is defined by

$$H_0^2(I) = \left\{ w \mid w \in H^2(I),\ w(0,t) = w(L,t) = 0,\ w_x(0,t) = w_x(L,t) = 0 \right\}. \tag{3.1}$$

For any $v(x) \in H_0^2(I)$ and the fixed t, multiply both sides of equation (2.1) by $v(x)$ and integrate over $(0,l)$, we have

$$\int_0^l \left[EIw_{xxxx} + \rho S w_{tt} - \rho I w_{xxtt} - P w_{xx} \right] v(x) \mathrm{d}x = \int_0^l f v(x) \mathrm{d}x. \tag{3.2}$$

By means of the boundary conditions (2.2) and the integration by parts, the integrals in (3.2) can be written as

$$\begin{aligned}
&\int_0^l EIw_{xxxx}v(x)\mathrm{d}x = -w_{xx}v_x\,|_0^l + \int_0^l EIw_{xx}v_{xx}(x)\mathrm{d}x = (EIw_{xx}, v_{xx}(x)),\\
&\int_0^l \rho Iw_{xxtt}v(x)\mathrm{d}x = \rho Iw_{xtt}v\,|_0^l - \int_0^l \rho Iw_{xtt}v_x(x)\mathrm{d}x = -(\rho Iw_{xtt}, v_x(x)),\\
&\int_0^l Pw_{xx}v(x)\mathrm{d}x = Pw_xv\,|_0^l - \int_0^l Pw_xv_x(x)\mathrm{d}x = -(Pw_x, v_x(x)),
\end{aligned} \tag{3.3}$$

where $(w, v) = \int_0^l wv\mathrm{d}x$.

Based on (2.3), the weak formulation of (2.1) is presented as

$$\begin{cases}
(EIw_{xx}, v_{xx}) + (\rho Sw_{tt}, v) + (\rho Iw_{xtt}, v_x) + (Pw_x, v_x) = (f(x,t), v),\ \forall v \in H_0^2,\\
w(x,0) = \varphi(x), w_t(x,0) = \psi(x),\ x \in [0,l].
\end{cases} \tag{3.4}$$

Given a positive integer M. Let $I_h : 0 = x_0 < x_1 < \cdots < x_M = l$ be an uniform partition of the interval $[0,l]$ with the step-size $h = l/M$, where $x_i = ih$, $i = 0, 1, 2, \cdots, M$. Let V_h be a subspace of $H_0^2(I)$ constituted by piecewise cubic Hermite type polynomials on I_h. Based on the above partition, the semi-discrete Galerkin finite element approximation of (3.4) can be define: find $w_h \in V_h$ such that

$$\begin{aligned}
&(EIw_{h,xx}, v_{h,xx}) + (\rho Sw_{h,tt}, v_h) + (\rho Iw_{h,xtt}, v_{h,x}) + (Pw_{h,x}, v_{h,x})\\
&= (f(x,t), v_h),\quad \forall v_h \in V_h.
\end{aligned} \tag{3.5}$$

We first discuss the Hermite interpolation problem in the reference interval $[0,1]$. Then, the interpolation problem in any interval $[x_i, x_{i+1}]$ can be solved by the coordinate transformation. The cubic basis functions in the reference interval $[0,1]$ are presented as

$$\begin{cases}
\alpha_0(\widehat{x}) = (2\widehat{x}+1)(1-\widehat{x})^2,\\
\beta_0(\widehat{x}) = \widehat{x}(1-\widehat{x})^2,
\end{cases}
\begin{cases}
\alpha_1(\widehat{x}) = (3-2\widehat{x})\widehat{x}^2,\\
\beta_1(\widehat{x}) = (\widehat{x}-1)\widehat{x}^2.
\end{cases} \tag{3.6}$$

Based on (3.6), basis functions in the interval $[x_i, x_{i+1}]$ can be obtained by using the coordinate transformation $\widehat{x} = \frac{x-x_n}{h}$ and are presented as follows

$$\begin{cases}
\alpha_i(x) = (2\dfrac{x-x_n}{h}+1)(1-\dfrac{x-x_n}{h})^2,\\
\beta_i(x) = \dfrac{x-x_n}{h}(1-\dfrac{x-x_n}{h})^2,
\end{cases}
\begin{cases}
\alpha_{i+1}(x) = (3-2\dfrac{x-x_n}{h})(\dfrac{x-x_n}{h})^2,\\
\beta_{i+1}(x) = (\dfrac{x-x_n}{h}-1)(\dfrac{x-x_n}{h})^2.
\end{cases} \tag{3.7}$$

where $\alpha_i(x)$ and $\beta_i(x)$ are equal to zero outside the interval $[x_{i-1}, x_{i+1}]$.

Because $w_h \in V_h$ in the semi-discrete finite element approximation (3.4), it is clear that w_h can be written as

$$w_h = \sum_{i=0}^{M} [w_i \alpha_i(x) + w_i^{'} \beta_i(x)], \tag{3.8}$$

where $w_i = w_h(x_i, t)$, $w_i' = w_h'(x_i, t)$.

We now present the main result in this paper.

Theorem 3.1. *Let $W = (w_1, \cdots, w_{M-1}, w_0', \cdots, w_M')^T$. Let F be the load vector, where $F = [(f, \alpha_1), \cdots, (f, \alpha_{M-1}), (f, \beta_0), \cdots, (f, \beta_M)]^T$. The vector W is the solution of the matrix differential equation*

$$A\frac{d^2W}{dt^2} + BW = F, \tag{3.9}$$

where matrices A and B are known sparse matrices.

Proof. It is clear that $\alpha_j(x) \in V_h$ and $\beta_j(x) \in V_h$. Set $v_h = \alpha_j(x)$. By substituting (3.8) into the semi-discrete finite element form (3.5), we obtain

$$\begin{aligned}
&\sum_{i}^{M} [\frac{d^2 w_i}{dt^2}(\rho S \alpha_i, \alpha_j) + \frac{d^2 w_i^{'}}{dt^2}(\rho S \beta_i, \alpha_j) + \frac{d^2 w_i}{dt^2}(\rho I \alpha_i^{'}, \alpha_j^{'}) + \frac{d^2 w_i^{'}}{dt^2}(\rho I \beta_i^{'}, \alpha_j^{'}) \\
&+ w_i(EI\alpha_i^{''}, \alpha_j^{''}) + w_i^{'}(EI\beta_i^{''}, \alpha_j^{''}) + w_i(P\alpha_i^{'}, \alpha_j^{'}) + w_i^{'}(P\beta_i^{'}, \alpha_j^{'})] \\
=&(f, \alpha_j),\ j = 0, 1, 2, \cdots, M.
\end{aligned} \tag{3.10}$$

Set $v_h = \beta_j(x)$. By substituting (3.8) into (3.5), we then obtain

$$\begin{aligned}
&\sum_{i}^{M} [\frac{d^2 w_i}{dt^2}(\rho S \alpha_i, \beta_j) + \frac{d^2 w_i^{'}}{dt^2}(\rho S \beta_i, \beta_j) + \frac{d^2 w_i}{dt^2}(\rho I \alpha_i^{'}, \beta_j^{'}) + \frac{d^2 w_i^{'}}{dt^2}(\rho I \beta_i^{'}, \beta_j^{'}) \\
&+ w_i(EI\alpha_i^{''}, \beta_j^{''}) + w_i^{'}(EI\beta_i^{''}, \beta_j^{''}) + w_i(P\alpha_i^{'}, \beta_j^{'}) + w_i^{'}(P\beta_i^{'}, \beta_j^{'})] \\
=&(f, \beta_j),\ j = 0, 1, 2, \cdots, M.
\end{aligned} \tag{3.11}$$

Let $W = (w_1, \cdots, w_{M-1}, w_0', \cdots, w_M')^T$. According to the boundary conditions (2.2), it is clear that $w_0 = 0$ and $w_M = 0$. Let $F = [(f, \alpha_1), \cdots, (f, \alpha_{M-1}), (f, \beta_0), \cdots, (f, \beta_M)]^T$ be the load vector. According to (3.10) and (3.11), we have

$$A\frac{d^2W}{dt^2} + BW = F, \tag{3.12}$$

where

$$A = \begin{pmatrix} A_{11} & A_{12} \\ A_{21} & A_{22} \end{pmatrix}_{2M \times 2M}, B = \begin{pmatrix} B_{11} & B_{12} \\ B_{21} & B_{22} \end{pmatrix}_{2M \times 2M}, \tag{3.13}$$

where

$$A_{11}=\begin{pmatrix}\rho S(\alpha_1,\alpha_1)+\rho I(\alpha_1^{'},\alpha_1^{'}) & \cdots & \rho S(\alpha_{M-1},\alpha_1)+\rho I(\alpha_{M-1}^{'},\alpha_1^{'})\\ \vdots & \ddots & \vdots\\ \rho S(\alpha_1,\alpha_{M-1})+\rho I(\alpha_1^{'},\alpha_{M-1}^{'}) & \cdots & \rho S(\alpha_{M-1},\alpha_{M-1})+\rho I(\alpha_{M-1}^{'},\alpha_{M-1}^{'})\end{pmatrix}_{(M-1)\times(M-1)}$$

$$A_{12}=\begin{pmatrix}\rho S(\beta_1,\alpha_1)+\rho I(\beta_1^{'},\alpha_1^{'}) & \cdots & \rho S(\beta_M,\alpha_1)+\rho I(\beta_M^{'},\alpha_1^{'})\\ \vdots & \ddots & \vdots\\ \rho S(\beta_1,\alpha_{M-1})+\rho I(\beta_1^{'},\alpha_{M-1}^{'}) & \cdots & \rho S(\beta_M,\alpha_{M-1})+\rho I(\beta_M^{'},\alpha_{M-1}^{'})\end{pmatrix}_{(M-1)\times(M+1)}$$

$$A_{21}=\begin{pmatrix}\rho S(\alpha_1,\beta_0)+\rho I(\alpha_1^{'},\beta_0^{'}) & \cdots & \rho S(\alpha_{M-1},\beta_0)+\rho I(\alpha_{M-1}^{'},\beta_0^{'})\\ \vdots & \ddots & \vdots\\ \rho S(\alpha_1,\beta_{M-1})+\rho I(\alpha_1^{'},\beta_M^{'}) & \cdots & \rho S(\alpha_{M-1},\beta_M)+\rho I(\alpha_{M-1}^{'},\beta_M^{'})\end{pmatrix}_{(M+1)\times(M-1)}$$

$$A_{22}=\begin{pmatrix}\rho S(\beta_0,\beta_0)+\rho I(\beta_0^{'},\beta_0^{'}) & \cdots & \rho S(\beta_M,\beta_0)+\rho I(\beta_M^{'},\beta_0^{'})\\ \vdots & \ddots & \vdots\\ \rho S(\beta_0,\beta_M)+\rho I(\beta_0^{'},\beta_M^{'}) & \cdots & \rho S(\beta_M,\beta_M)+\rho I(\beta_M^{'},\beta_M^{'})\end{pmatrix}_{(M+1)\times(M+1)} \tag{3.14}$$

$$B_{11}=\begin{pmatrix}EI(\alpha_1^{''},\alpha_1^{''})+P(\alpha_1^{'},\alpha_1^{'}) & \cdots & EI(\alpha_{M-1}^{''},\alpha_1^{''})+P(\alpha_{M-1}^{'},\alpha_1^{'})\\ \vdots & \ddots & \vdots\\ EI(\alpha_1^{''},\alpha_{M-1}^{''})+P(\alpha_1^{'},\alpha_{M-1}^{'}) & \cdots & EI(\alpha_{M-1}^{''},\alpha_{M-1}^{''})+P(\alpha_{M-1}^{'},\alpha_{M-1}^{'})\end{pmatrix}_{(M-1)\times(M-1)}$$

$$B_{12}=\begin{pmatrix}EI(\beta_1^{''},\alpha_1^{''})+P(\beta_1^{'},\alpha_1^{'}) & \cdots & EI(\beta_M^{''},\alpha_1^{''})+P(\beta_M^{'},\alpha_1^{'})\\ \vdots & \ddots & \vdots\\ EI(\beta_1^{''},\alpha_{M-1}^{''})+P(\beta_1^{'},\alpha_{M-1}^{'}) & \cdots & EI(\beta_M^{''},\alpha_{M-1}^{''})+P(\beta_M^{'},\alpha_{M-1}^{'})\end{pmatrix}_{(M-1)\times(M+1)}$$

$$B_{21}=\begin{pmatrix}EI(\alpha_1^{''},\beta_0^{''})+P(\alpha_1^{'},\beta_0^{'}) & \cdots & EI(\alpha_{M-1}^{''},\beta_0^{''})+P(\alpha_{M-1}^{'},\beta_0^{'})\\ \vdots & \ddots & \vdots\\ EI(\alpha_1^{''},\beta_{M-1}^{''})+P(\alpha_1^{'},\beta_M^{'}) & \cdots & EI(\alpha_{M-1}^{''},\beta_M^{''})+P(\alpha_{M-1}^{'},\beta_M^{'})\end{pmatrix}_{(M+1)\times(M-1)}$$

$$B_{22}=\begin{pmatrix}EI(\beta_0^{''},\beta_0^{''})+P(\beta_0^{'},\beta_0^{'}) & \cdots & EI(\beta_M^{''},\beta_0^{''})+P(\beta_M^{'},\beta_0^{'})\\ \vdots & \ddots & \vdots\\ EI(\beta_0^{''},\beta_M^{''})+P(\beta_0^{'},\beta_M^{'}) & \cdots & EI(\beta_M^{''},\beta_M^{''})+P(\beta_M^{'},\beta_M^{'})\end{pmatrix}_{(M+1)\times(M+1)}. \tag{3.15}$$

When $|i-j|>1$, x_i and x_j are not neighboring mesh nodes. Hence in the interval $[x_i,x_{i+1}]$, α_j and β_j are euqal to 0. It is clear that most of the elements

a_{ij} in matrix A are equal to 0. Hence the stiffness matrix A is the sparse matrix. Similarly, the matrix B is also the sparse matrix. The proof is completed. □

Remark 3.1. Once the vector W is obtained, the numerical solutions at all the mesh nodes and the finite element solution $w_h = \sum_{i=0}^{M} [w_i\alpha_i(x) + w_i^{'}\beta_i(x)]$ are obtained. Therefore, the numerical solutions of the weak formulation (3.4) can be obtained by solving the matrix differential equation (3.9).

Remark 3.2. Compared with traditional finite element method, the Hermite finite element method can guarantee the continuity of the first derivative of the interpolation function. And the Hermite finite element method has a better approximation for the derivatives of solution within each element. Therefore, Hermite elements can provide higher accuracy with fewer elements than standard Lagrange elements.

Given a positive integer N. Let $0 = t_0 < t_1 < \cdots < t_N = T$ be an uniform partition of the interval $[0, T]$ with the step-size $\tau = T/N$, where $T > 0$ is a constant and $t_n = n\tau$, $n = 0, 1, 2, \cdots, N$. By applying the central difference scheme to discretize $\frac{d^2W}{dt^2}$, the full-discrete finite element form of problem (3.4) can be define: find $w_h^n \in V_h$ such that

$$(EIw_{h,xx}^{n+1}, v_{h,xx}) + (\rho S\frac{w_h^{n+1} - 2w_h^n + w_h^{n-1}}{\tau^2}, v_h) + (\rho I\frac{w_{h,x}^{n+1} - 2w_{h,x}^n + w_{h,x}^{n-1}}{\tau^2}, v_{h,x}) + (Pw_{h,x}^{n+1}, v_{h,x}) = (f^{n+1}(x,t), v_h), \forall v_h \in V_h. \tag{3.16}$$

The numerical algorithm based on the Hermite finite element method is developed to solve the fourth-order Rayleigh-Bishop equation (2.1).

Algorithm 1 A numerical algorithm for the Rayleigh-Bishop equation

1: Initialization: Given constants $T > 0$ and $l > 0$. Given positive integers N and M. Initialize matrices $A = \mathbf{0}_{2M\times 2M}$, $B = \mathbf{0}_{2M\times 2M}$ and the load vector $F = \mathbf{0}_{2M}$

2: Compute matrices A_{11},A_{12},A_{21} and A_{22} in (3.14) and assemble them into matrix A. Compute matrices B_{11},B_{12},B_{21} and B_{22} in (3.15) and assemble them into matrix B. Compute the inner products (f, α_i) and (f, β_j) and assemble them into the load vector F, where $i = 1, \cdots, M-1$ and $j = 0, \cdots, M$.

3: Let $W^{n+1} = (w_1^{n+1}, \cdots, w_{M-1}^{n+1}, w_0^{'n+1}, \cdots, w_M^{'n+1})^T$. By means of the iterative method, W^{n+1} is obtained by solving the following algebraic equation

$$(A + B\tau^2)W^{n+1} = \tau^2 F^{n+1} + 2AW^n - AW^{n-1}.$$

The coefficient w_i^{n+1} is the numerical solution of node x_i at time t_{n+1}.

4: Calculate the numerical solution w_h^n by substituting w_i^n and $w_i^{'n}$ into the following euqation

$$w_h^n = \sum_{i=0}^{M} [w_i^n\alpha_i(x) + w_i^{'n}\beta_i(x)].$$

Remark 3.3. The numerical algorithm based on the Hermite finite element method provides piecewise functions defined on the whole problem domain as numerical solutions, not just the numerical solutions at mesh nodes.

4. Numerical Examples

In this section, we give one example to demonstrate the effectiveness of the proposed method. The exact solution of this example is given. We apply Algorithm 1 proposed above to calculate the numerical solution of the example.

Example 4.1. Let the variables E, I,P, ρ, S, l and P in problem (2.1) be equal to 1. Consider the following initial-boundary value problem:

$$\begin{cases} w_{xxxx} + w_{tt} - w_{xxtt} - w_{xx} = 0, \ x \in (0,1), t \in (0,1], \\ w(x,0) = \sin(\pi x), w_t(x,0) = 0, \ x \in [0,1], \\ w(0,t) = w(1,t) = 0, w_{xx}(0,t) = w_{xx}(1,t) = 0, \ t \in [0,1]. \end{cases} \tag{4.1}$$

The exact solution is $w(x,t) = \sin(\pi x)\cos(\pi t)$.

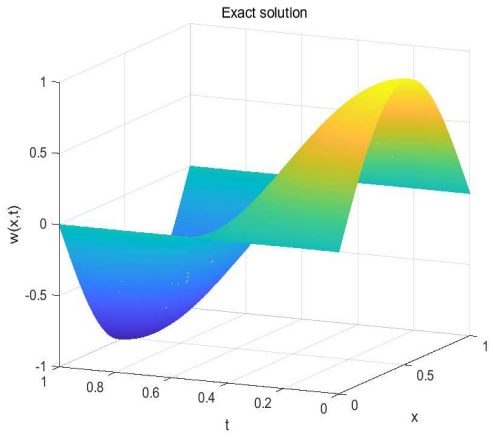

Figure 2. The exact solution with $h = 0.01$ and $\tau = 0.0001$.

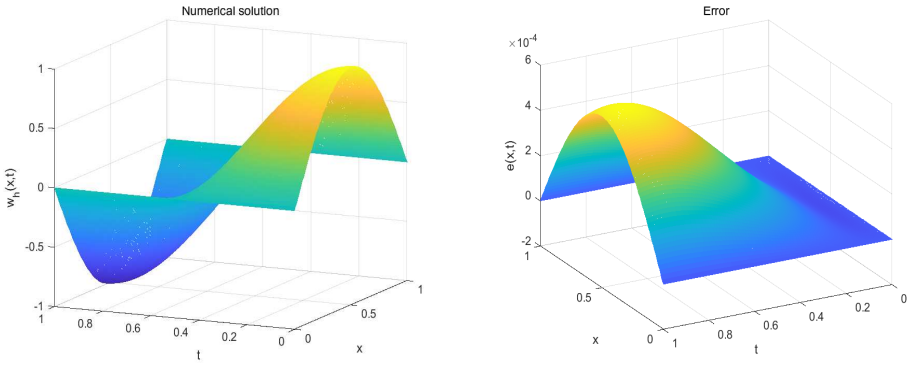

(a) (b)

Figure 3. The numerical solution and the error of the fully discrete scheme with $h = \frac{1}{10^2}$ and $\tau = \frac{1}{10^4}$.

The exact solution to the problem (4.1) is shown in Figure 2. To demonstrate the effectiveness of the proposed numerical method, we use Algorithm 1 to solve

the problem (4.1). The numerical solution of the problem (4.1) is shown in Figure 3(a). Let $e(x,t)$ be the error between the exact solutions and numerical solutions. The error $e(x,t)$ of the fully discrete scheme with $h=\frac{1}{10^2}$ and $\tau=\frac{1}{10^4}$ is shown in Figure 3(b). In Table 1, We present the L^2-error at different time steps and space steps. The results show that the space convergence order of the proposed scheme is higher than the convergence order in time.

Table 1. Example 4.1: Errors of numerical solutions.

h	τ	L^2-error
0.1	0.01	6.7371e-04
0.1	0.001	2.6447e-05
0.1	0.0001	2.0000e-05
0.01	0.1	0.0486
0.01	0.01	5.9182e-04
0.01	0.001	6.1075e-06
0.01	0.0001	6.9603e-08

Remark 4.1. When $h=0.1$ and $\tau=0.01$, the L^2-error is $6.7371e-04$. When $h=0.01$ and $\tau=0.1$, the L^2-error is 0.0486. It is clear that the space convergence order of the proposed scheme is higher than the convergence order in time.

Example 4.2. Let the bending stiffness $EI=1.00N\cdot m^2$, the rotatory inertia of cross-sectional area $\rho I=4.00kg\cdot m$, the mass per unit length $\rho S=4.00kg/m$, the coefficient of tension $P=1.00N$ and $l=1.00m$ in problem (2.1). Consider the following initial-boundary value problem:

$$\begin{cases} w_{xxxx}+4w_{tt}-4w_{xxtt}-w_{xx}=0,\ x\in(0,1), t\in(0,1], \\ w(x,0)=\sin(2\pi x), w_t(x,0)=0,\ x\in[0,1], \\ w(0,t)=w(1,t)=0, w_{xx}(0,t)=w_{xx}(1,t)=0,\ t\in[0,1]. \end{cases} \tag{4.2}$$

The exact solution is $w(x,t)=\sin(2\pi x)\cos(\pi t)$.

We present the exact solution for problem (4.2) in Figure 4. To assess the effectiveness of our proposed numerical method, we employ Algorithm 1 to solve the problem (4.2). The resulting numerical solution is visualized in Figure 5(a). Figure 5(b) illustrates the error $e(x,t)$ of the fully discrete scheme for a specific case with $h=\frac{1}{10^2}$ and $\tau=\frac{1}{10^4}$. A more detail information of the error is provided in Table 2 which presents the L^2-error at different time steps and space steps. The results show that the space convergence order of the proposed scheme is higher than the convergence order in time.

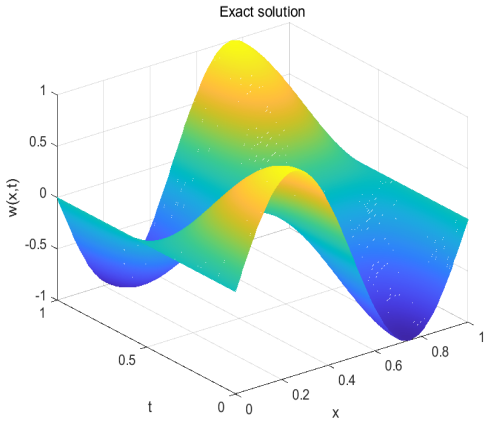

Figure 4. The exact solution with $h = 0.01$ and $\tau = 0.0001$.

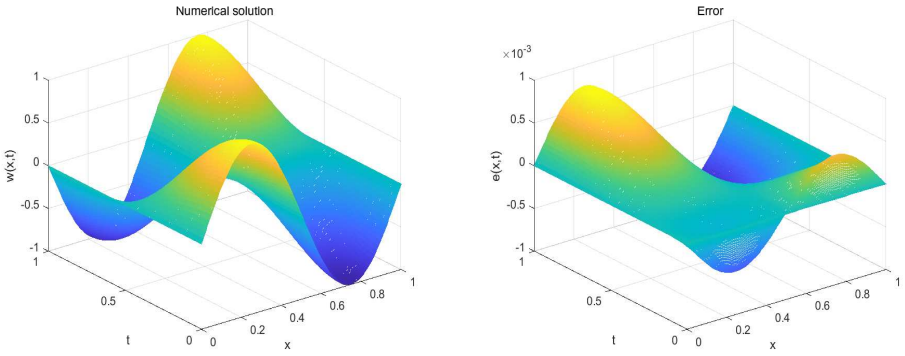

(a) (b)

Figure 5. The numerical solution and the error of the fully discrete scheme with $h = \frac{1}{10^2}$ and $\tau = \frac{1}{10^4}$.

Table 2. Example 4.2: Errors of numerical solutions.

h	τ	L^2-error
0.1	0.01	1.0000e-03
0.1	0.001	3.0313e-04
0.1	0.0001	2.7943e-04
0.01	0.1	0.0506
0.01	0.01	5.9403e-04
0.01	0.001	6.3647e-06
0.01	0.0001	1.1125e-07

5. Conclusion

In this paper, we present a Hermite finite element method for the vibration problem of the Rayleigh-Bishop beam. Based on the Galerkin variational method, the semi-discrete finite element form for the Rayleigh-Bishop equation is established. Then by means of the cubic Hermite element, a full-discrete finite element scheme is presented, which can guarantee the continuity of the first derivative of the interpolation function. Then, a numerical algorithm , Algorithm 1, is developed to solve the fourth-order Rayleigh-Bishop equation. Finally, the effectiveness of Algorithm 1 is verified by a numerical example. The proposed method is potentially applied to other vibration problems.

References

[1] S. R. Singiresu, *Vibration of Continuous Systems*, Hoboken, NJ, USA: John Wiley & Sons, 2019.

[2] F. Igor, S. Michael and M. Julian, *Hyperbolic and pseudo-hyperbolic equations in the theory of vibration*, Acta Mechanica, 2016, 227, 3315–3324.

[3] Y. Wang, H. Ding and L. Q. Chen, *Vibration of axially moving hyperelastic beam with finite deformation*, Applied Mathematical Modelling, 2019, 71, 269–285.

[4] C. Yu, J. Zhang, Y. Chen, Y. Feng and A. Yang, *A numerical method for solving fractional-order viscoelastic Euler-Bernoulli beams*, Chaos, Solitons & Fractals, 2019, 128, 275–279.

[5] A. C. Galucio, J. F. Deü and R. Ohayon, *Finite element formulation of viscoelastic sandwich beams using fractional derivative operators*, Computational Mechanics, 2004, 33, 282–291.

[6] J. Niiranen, V. Balobanov, J. Kiendl and S. Hosseini, *Variational formulations, model comparisons and numerical methods for Euler-Bernoulli micro-and nano-beam models*, Mathematics and Mechanics of Solids, 2019, 24, 312–335.

[7] A. Dabbagh, A. Rastgoo and F. Ebrahimi, *Finite element vibration analysis of multi-scale hybrid nanocomposite beams via a refined beam theory*, Thin-Walled Structures, 2019, 140, 304–317.

[8] E. Carrera and D. Scano, *Finite elements based on Jacobi shape functions for the free vibration analysis of beams, plates, and shells*, Mechanics of Advanced Materials and Structures, 2024, 31, 4–12.

[9] H. Guo, S. Lin and H. Zheng, *GMLS-based numerical manifold method in mechanical analysis of thin plates with complicated shape or cutouts*, Engineering Analysis with Boundary Elements, 2023, 151, 597–623.

[10] H. Guo, X. Cao, Z. Liang, S. Lin, H. Zheng and H. Cui, *Hermitian numerical manifold method for large deflection of irregular Föppl-von Kármán plates*, Engineering Analysis with Boundary Elements, 2023, 153, 25–38.

[11] Z. Chen, Z. Yang, N. Guo and G. Zhang, *An energy finite element method for high frequency vibration analysis of beams with axial force*, Applied Mathematical Modelling, 2018, 61, 521–539.

[12] H. Elhuni and D. Basu, *Dynamic soil structure interaction model for beams on viscoelastic foundations subjected to oscillatory and moving loads*, Computers and Geotechnics, 2019, 115, 103157.

[13] R. L. Taylor, F. C. Filippou, A. Saritas and F. Auricchio, *A mixed finite element method for beam and frame problems*, Computational Mechanics, 2003, 31, 192–203.

[14] C. Chazal and R. M. Pitti, *Integral approach for time dependent materials using finite element method*, Journal of Theoretical and Applied Mechanics, 2011, 49, 1029–1048.

[15] F. P. Pinnola, M. S. Vaccaro, R. Barretta and F. M. de Sciarra, *Finite element method for stress-driven nonlocal beams*, Engineering Analysis with Boundary Elements, 2022, 134, 22–34.

[16] E. D. Sánchez, L. G. Nallim, F. J. Bellomo and S. H. Oller, *Generalized viscoelastic model for laminated beams using hierarchical finite elements*, Composite Structures, 2022, 235, 111794.

[17] Y. Tang and Z. Yin, *Hermite finite element method for a class of viscoelastic beam vibration problem*, Engineering, 2021, 13, 463–471.

[18] K. Koutoati, F. Mohri and E. Carrera, *A finite element approach for the static and vibration analyses of functionally graded material viscoelastic sandwich beams with nonlinear material behavior*, Composite Structures, 2021, 274, 114315.

[19] B. Deka, P. Roy and N. Kumar, *Weak Galerkin finite element methods combined with Crank-Nicolson scheme for parabolic interface problems*, Journal of Applied Analysis and Computation, 2020, 10, 1433–1442.

[20] H. Liu and P. Huang, *A two-grid decoupled finite element method for the stationary closed-loop geothermal system*, Journal of Applied Analysis and Computation, 2023, 13, 1837–1851.

[21] J. Marais, I. Fedotov and M. Shatalov, *Longitudinal vibrations of a cylindrical rod based on the Rayleigh-Bishop theory*, Afrika Matematika, 2015, 26, 1549–1560.

[22] I. A. Fedotov, A. D. Polyanin, M. Y. Shatalov and H. M. Tenkam, *Longitudinal vibrations of a Rayleigh-Bishop rod*, Doklady Physics, 2010, 55, 609–614.

[23] G. V. Demidenko and S. V. Upsenskii, *Partial differential equations and systems not solvable with respect to the highest-order derivative*. New York: Marcel Dekker, 2003.

[24] G. V. Demidenko, *Solvability conditions of the Cauchy problem for pseudohyperbolic equations*, Siberian Mathematical Journal, 2015, 56, 1028–1041.

[25] L. N. Bondar and G. V. Demidenko, *Solvability of the Cauchy problem for a pseudohyperbolic system*, Complex Variables and Elliptic Equations, 2021, 66, 1084–1099.

[26] H. Guo and H. Rui, *Least-squares Galerkin procedures for pseudohyperbolic equations*, Applied Mathematics and Computation, 2007, 189, 425–439.

[27] Y. Liu and H. Li, *H^1-Galerkin mixed finite element methods for pseudohyperbolic equations*, Applied Mathematics and Computation, 2009, 212, 446–457.

[28] M. Shatalov, J. Marais, I. Fedotov, M. D. Tenkam and M. Schmidt, *Longitudinal vibration of isotropic solid rods: from classical to modern theories*, Advances in Computer Science and Engineering, 2011, 212, 187–214.